Results of Tests and Simulations for the Top Counting Detector and Bottom Counting Detector of the ISS-CREAM Experiment

J. M. PARK[1], T. ANDERSON[2], D. ANGELASZEK[3], J. B. BAE[1], S. J. BAEK[4], J. BAYLON[5], M. COPLEY[3], S. COUTU[2], M. GUPTA[3], J. H HAN[3], H. G. HUH[3], Y. S. HWANG[1], H. J. HYUN[1], I. S. JEONG[4], D. H. KAH[1], K. H. KANG[1], H. J. KIM[1], K. C. KIM[3], K. KWASHNAK[3], J. LEE[4], M.H LEE[3], J. T. LINK[6,7], L. LUTZ[3], A. MALININ[3], A. MENCHACA-ROCHA[5], J. W. MITCHELL[6], S. NUTTER[8], O. OFOHA[3], H. PARK[1], I. H. PARK[4], P. PATTERSON[3], E. S. SEO[3], J. WU[3], Y. S. YOON[3].

[1] *Kyungpook National University, Deagu 702-701, South Korea*
[2] *Pennsylvania State University, University Park, PA 16802, USA*
[3] *University of Maryland, College Park, MD 20740, USA*
[4] *Sungkyunkwan University, Suwon 440-746, South Korea*
[5] *Universidad Nacional Autonoma de Mexico, Mexico*
[6] *NASA GSFC, Columbia, MD 20771, USA*
[7] *CRESST(USRA), MD 21044, USA*
[8] *Northern Kentucky University, Highland Heights, KY 41099, USA*

hongjooknu@gmail.com

Abstract: The cosmic-ray elemental spectrum is important to understand the generation and acceleration mechanism of high-energy cosmic rays. The Cosmic Rays Energetics And Mass (CREAM) experiment on the International Space Station (ISS) plans to measure nuclear and electron energy spectra precisely. The separation of electrons from protons is crucial because the proton flux is about 1000 times higher than that of electrons in the energy range 300 GeV $\sim$ 800 GeV. The Top Counting Detector (TCD) and Bottom Counting Detector (BCD) are designed to optimize e/p separation. The TCD and BCD each consists of a plastic scintillator and an average of 400 photo-diodes, respectively. The TCD and BCD are located immediately above and below the calorimeter, respectively. This detector configuration provides e/p separation by using the different shapes of electromagnetic and hadronic showers. We have characterized the performance of the TCD/BCD in several different ways. The signal to noise ratio of the detector cell components was measured by using a ^{90}Sr radioactive source and a high-energy beam at CERN. The temperature dependence of the detector cell component, from -40 °C to 70 °C, and the robustness of the TCD/BCD module were confirmed using thermal and vacuum chambers. We present the TCD/BCD design considerations and a summary of the measured performance of the TCD/BCD modules.

Keywords: CREAM, TCD/BCD, e/p separation.

1 Introduction

The origin of cosmic rays remains poorly understood but, steady progress is being accomplished in refining the long-standing paradigm of acceleration in association with supernova shocks in the galaxy [1-4]. To this end it is particularly important to push the direct measurement of the elemental spectra with balloon and space-based instruments into the 10^{14} - 10^{15} eV region, to provide overlap with indirect studies with ground-based instruments.

The CREAM experiment will be installed on the ISS in 2014 [5]. ISS-CREAM plans to measure nuclear and electron energy spectra precisely. Primary cosmic rays consist mainly of protons and helium nuclei, but also include a small leptonic component. The latter amounts to only 10^{-2} - 10^{-3} of the flux, and positrons amount to only about 10% of the leptonic component. Therefore, the separation of electrons from the large proton background is crucial for studying the high energy electron cosmic rays spectrum [6, 7]. ISS-CREAM comprises a Silicon Charge Detector (SCD), a carbon target, a tungsten/scintillator sampling calorimeter, a Top Counting Detector, a Bottom Counting Detector and a Boronated Scintillator Detector (BSD).

The TCD/BCD are designed to optimize e/p separation by using the different shapes of electromagnetic and hadronic showers. These detectors each consists of a plastic scintillator and an array of 400 photo-diodes. The dimensions for the TCD and BCD are 900 × 535 × 30 mm^3 and 950 × 651 × 33 mm^3, respectively. The TCD is located between the instrument's carbon target and the calorimeter, and the BCD is located below the calorimeter. We have characterized the performance of the TCD/BCD in several different ways. We tested the performance of the custom developed photo-diode of dimensions 2.3 × 2.3 cm^2. The signal to noise ratio (SNR) of the detector's cell components was measured by using a ^{90}Sr radioactive source and a high-energy beam at CERN. Since the ISS-CREAM detectors need to survive in a temperature range from -40 °C to 70 °C, the temperature dependence of the detector cell component and the robustness of the TCD/BCD module were tested using thermal and vacuum chambers.

2 Measurement System and Results

2.1 Design of TCD/BCD

The TCD/BCD are designed to optimize electron and proton (e/p) separation by using the different shapes of electromagnetic and hadronic showers. Both detectors consist of a polyvinyltoluene plastic scintillator (EJ-200) from Eljen Technologies. and an array of 400 photo-diodes. The photo-diode (PD) was custom developed at Kyungpook National University. The PD is 650 μm thick and uses n-type silicon wafers. The full depletion voltage of the bulk capacitance was measured to be below -250 V and the leakage current below 20 nA/cm^2 at operating voltage. As shown in Fig. 1, the enclosures of the TCD/BCD are made using Aluminum (6061Alloy) and the dimensions are 900 $\times$ 535 $\times$ 30 mm^3 and 950 $\times$ 651 $\times$ 33 mm^3, respectively. The masses of the TCD/BCD are 13 kg and 16 kg, respectively. Since the TCD/BCD need to survive under the launch conditions, a detailed mechanical simulation of stress and vibration conditions is crucial. The mechanical properties of the TCD/BCD are simulated for launch conditions using the SolidWorks program [8].

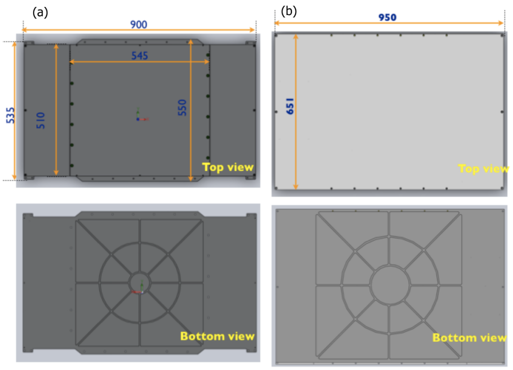

Fig. 1: Schematics of the (a) TCD and (b) BCD enclosures.

2.2 Radioactive Source Test

We used a ^{90}Sr radioactive source for measuring the SNR. Figure 2 shows the experimental set-up for the SNR measurement. The PD is used for test and a Hamamatsu Photonics photomultiplier tube (PMT, HM7400U) is used for the trigger. The polyvinyltoluene plastic scintillator (EJ-200) with the dimensions 20 $\times$ 20 $\times$ 5 mm^3 was attached to the PMT. The PD was attached to a printed circuit board, and was placed such that it faced the ^{90}Sr source on one side and the plastic scintillator on the other side. A lead collimator with 1 mm diameter hole was placed between the radioactive source and the PD. The PD was read out with a home made charge amplifier (AMP), an ORTEC 570 shaping AMP, and a home-made 25 MHz Flash Analog to Digital Converter (FADC). A trigger signal from the gate generator was transmitted to the trigger input of the FADC. We supplied a high voltage of -700 V to the PMT and the AMP shaping time, coarse gain, and fine gain were set at 3 μs, 50 and 0.5, respectively [9, 10].

We supplied a high voltage of -190 V to the PD. The SNR was defined as

$$SNR = (MPV - ped)/sigma\_pedestal$$

where MPV is the most probable value of the signal, ped is the mean value of the noise and sigma_pedestal is the width of the noise distribution, and measured to be 13.0 as shown in Fig. 3.

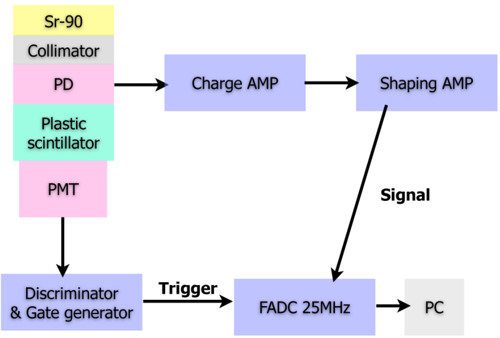

Fig. 2: Block diagram of the SNR measurement system.

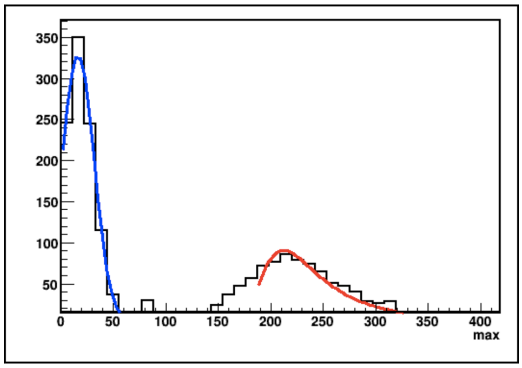

Fig. 3: Signal-to-noise ratio distribution obtained with the ^{90}Sr radioactive source.

2.3 Thermal/Vacuum test of the detector cell components

The TCD/BCD need to survive over an extreme temperature range from -40 °C to 70 °C. We measured the pedestal of the detector cell component which consists of one PD and plastic scintillator during a full thermal cycle. The measurement system was similar to that used for the SNR measurement. Since we measured only the pedestal of the detector cell component during the thermal cycle, we didn't use the trigger system. As shown in Fig. 4, the detector cell component and the AMP were both placed in the thermal chamber.

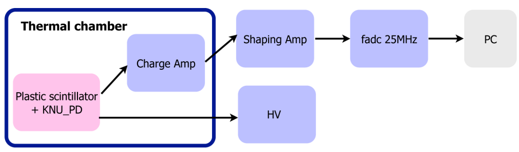

Fig. 4: Detector cell components used for the thermal test.

We ran a number of thermal cycles over an 11 hour period. We supplied a high voltage of -120 V to the detector cell components, and measured the pedestal without the radioactive source. We also carried out a calibration test, to find the e$^-$ RMS value that corresponds to one ADC count. As a result, one ADC count of the detector cell components corresponds to an RMS of 2083 e$^-$. As shown in Fig. 5, the value of e$^-$ RMS reliably tracked the temperature change.

Since the TCD/BCD need to survive an environmental vacuum of 10^{-5} torr, the detector cell component was maintained at 10^{-5} torr for 4 hours. The electrical charac-

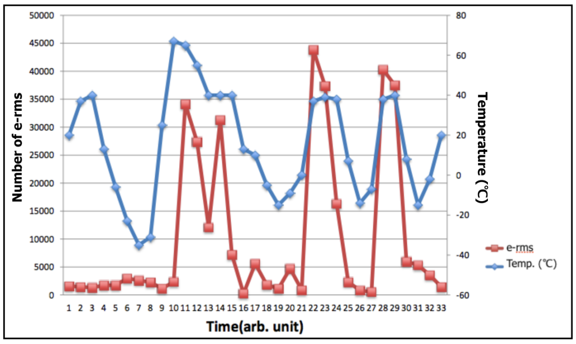

Fig. 5: Thermal test result of the detector cell component.

teristics of the detector cell component were measured before and after the vacuum test using a Keithley 6517 picoammeter and an HP 4277A LCZ meter [10].

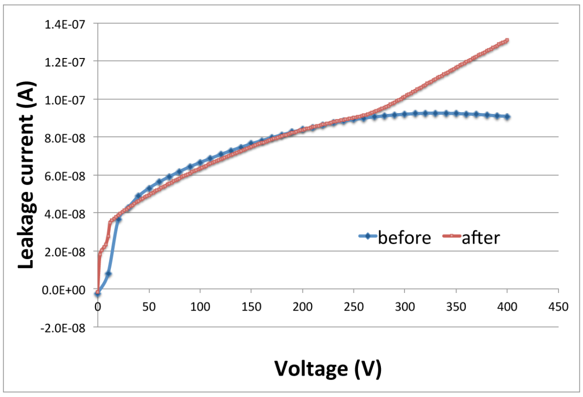

Fig. 6: I-V curve of the detector cell component before/after vacuum test.

As shown in Fig. 6, the leakage current values before and after the vacuum test were similar under a -250 V bias.

2.4 CERN Beam Test

We measured the performance of the TCD/BCD prototype using electron, muon and pion beams at CERN. Fig. 7 shows a schematic diagram of the system. As shown in Fig. 8, the prototype TCD/BCD had 32 PD channels attached to an EJ-200 plastic scintillator, each photo-diode of dimensions 23 mm $\times$ 23 mm. The signals from the 32 channel photo-diode being array were transmitted to a VA-TA Hybrid board. A Xilinx DAQ board digitized the signals which were analyzed offline using the ROOT package [10]. Control signals from the DAQ board were passed through logic converters and distributed to the VATA Hybrid board. The VATA has 128 channels but we used only 32 channels at CERN. Each channel consisted of a low noise charge sensitive preamplifier, a shaper, and a sample and hold circuit. A low voltage power supply provided the voltage to the VATA and DAQ boards, and the high voltage for the sensor was generated by an EMCO DC to HV DC converter.

One of the goals of the TCD/BCD is that it could provide a Minimum Ionizing Particle (MIP) trigger for calibration of the SCD and TCD/BCD. A MIP was measured by using punch through muons from the CERN beam. We recorded 50,000 signal events and 2000 pedestal events

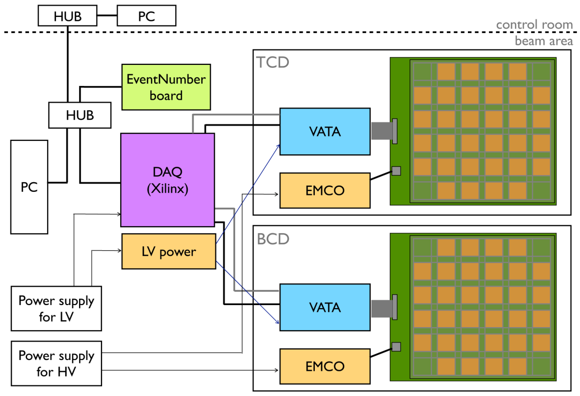

Fig. 7: Block diagram of the CERN beam test system.

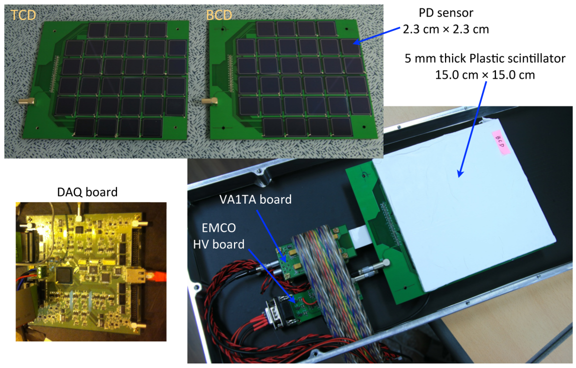

Fig. 8: Prototype TCD/BCD for the CERN beam test.

during the CERN beam test. As shown in Fig. 9, the SNR was measured to be 7.1 on average. Since the SNR needs to exceed 5 for MIP identification, the prototype TCD showed good performance for MIP identification

3 Conclusion

We fabricated the PD for the TCD/BCD and attached it to the plastic scintillator. The TCD/BCD will measure the high cosmic electron by providing e/p separation for ISS-CREAM. The SNR of the detector cell component was measured to be 13.0 with a ^{90}Sr radioactive source. The characteristics of the detector cell component were measured before/after thermal and vacuum tests. The value of the e^- RMS tracked well with temperature change. The leakage current value before/after the vacuum test did not change. Prototypes of the TCD/BCD were tested with a muon beam at CERN. The SNR of the prototype TCD/BCD was measured to be 7.1 on average which proves that the TCD/BCD can provide a MIP trigger for detector calibration.

Acknowledgment: The authors thank NASA Goddard Space Flight Center (GSFC) Wallops Flight Facility for project management and engineering support, and NASA Johnson Space Center ISS Program Office for the launch support and the ISS accommodation. This works was supported in the U.S. by NASA grants NNX11AC52G, NNX08AC15G, NNX08AC16G and their predecessor grants, as well as by directed RTOP funds to the NASA GSFC. It is supported in Korea by the Creative Research Initiatives of MEST/NRF and by a National Research Froundation (NRF) of Korea grant funded (NRF-2011-0016260, NRF-2011-0021196).

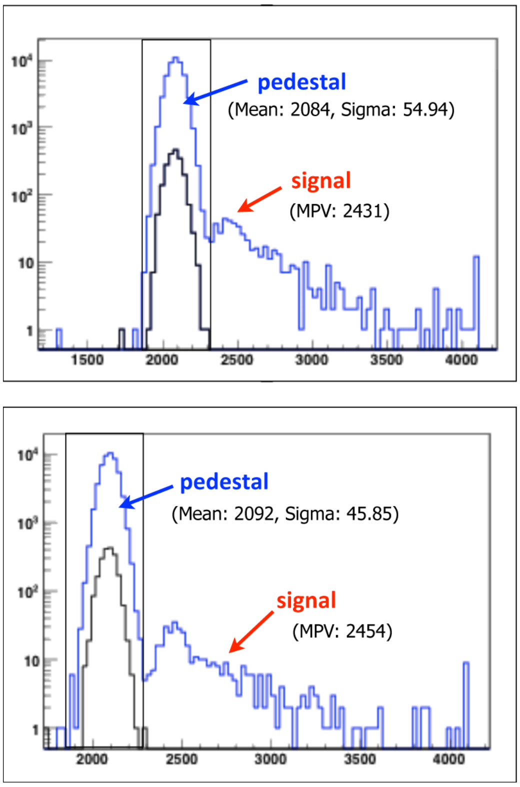

Fig. 9: Pulse-height distribution of two channels on the prototype BCD at the CERN beam test.

References

[1] E. S. Seo et al., Advances in Space Research 33 (2004) 1777-1785 doi:10.1016/j.asr.2003.05.019.
[2] Antje Putze, Nuclear Instruments and Methods in Physics Research A 662 (2012) S157-S163 doi:10.1016/j.nima.2010.11.133.
[3] H. S. Ahn et al., Nuclear Instruments and Methods in Physics Research A 579(2007) 1034-1053 doi:10.1016/j.nima.2007.05.203.
[4] O. Ganel et al., Czechoslovak Journal of Physics 56 (2006) A301-A312 doi:10.1007/s10582-006-0164-9.
[5] E. S. Seo et al., ID 0629 (2013) this conference.
[6] S A Voronov, S V Borisov and A V Karelin, Physics Uspekhi 52 (2009) 879-890 doi:10.3367/UFNe.0179.200909b.0931.
[7] V. I. Zatsepin, A. D. Panov and N. V. Sokolskaya, 32nd International Cosmic Ray Conference, Beijing 2011 6 (2011) 13 doi:10.7529/ICRC2011/V06/0277.
[8] http://www.solidworks.com
[9] H. J. Hyun et al., 2006 IEEE Nuclear Science Symposium Conference Record (2006) 713 doi:1-4244-0561-0.
[10] H. J. Hyun et al., 2011 IEEE Nuclear Science Symposium Conference Record (2011) 1076 doi:978-1-4673-0120-6.